symmetry

MDPI

Article

Docking of Polyethylenimines Derivatives on Cube Rhombellane Functionalized Homeomorphs

Beata Szefler * and Przemysław Czeleń

Department of Physical Chemistry, Faculty of Pharmacy, Collegium Medicum, Nicolaus Copernicus University, Kurpińskiego 5, 85-096 Bydgoszcz, Poland

* Correspondence: beatas@cm.umk.pl

Received: 22 July 2019; Accepted: 7 August 2019; Published: 14 August 2019

Abstract: Nowadays, in the world of science, an important goal is to create new nanostructures that may act as potential drug carriers. Among different, real or hypothetical, polymeric networks, rhombellanes are very promising and, therefore, attempts were made to deposit polyethylenimines as possible nano-drug complexes on the cube rhombellane homeomorphs surface. For the search of ligand–fullerene interactions, was used AutoDockVina software. As a reference structure, the fullerene C_{60} was used. After the docking procedure, the ligands–fullerenes interactions were tested. The important factor determining the mutual affinity of the tested ligands and nanocarriers is the symmetry of the analyzed nanostructures. Here, this feature has the influence on the distribution of such groups like donors and acceptors of hydrogen bonds on the surface of nanoparticles. We calculated the best binding affinities of ligands, values of binding constants and differences relative to C_{60} molecules. The best binding efficiency was found for linear ligands. It was also found that the shorter the molecule, the better the binding performance, the more the particle grows and the lower the yield. Small structures of ligands react easily with small structures of nanoparticles. The highest positive percentage deviations were obtained for ligand–fullerene complexes showing the highest binding energy values. Detailed analysis of structural properties after docking showed that the values of affinity of the studied indolizine ligands to the rhombellanes surface are correlated with the strength/length of hydrogen bonds formed between them.

Keywords: cube rhombellane homeomorph; PEI; polyethylenimines; nanostructure; molecular docking; affinity

1. Introduction

The development of multifunctional nanoparticles has a huge impact on the future of personalized medicine. Nanoparticles can be used for therapeutic purposes in anti-cancer therapy at the molecular level, which has been difficult so far. In earlier work [1–3], an enzyme GOx (3QVR) that fulfills the role of a biosensor, had been used for immobilization on the gel, while the polymer was polyethylenimine (PEI). By assembling polymeric nano-gels (for example PEI) and antibodies on nano-molecules [1–3], it was possible to recognize receptors of certain integrins on lung cancer tissues and to identify new cancer vessels.

In the present article, polyethylenimines (PEI) were studied. Molecular docking analysis of fifteen PEI derivatives acting as ligands on some cube rhombellane homeomorphs was carried out for the first time. Fourteen types of cube rhombellanes and three groups of polyethylenimines (PEIs), namely, branched (B-PEI), linear (L-PEI) and dendrimer (D-PEI) were used.

The choice of ligands and docked nanostructures was guided by our earlier studies [1–8].

PEIs (polyethylenimines) are polymeric molecules built of two aliphatic carbons and repeating units of amine groups. There are L-, B-, and DPEI (Figure 1). Linear PEI (LPEI) are built of secondary

and primary amino groups (Figure 1, left); branched PEI (B-PEI) are built of all types amino groups such as primary, secondary and tertiary (Figure 1, middle), while dendrimers [9,10] are symmetric around the core (Figure 1, right). PEI despite the fact that are cytotoxic [11], have many applications, first of all, as transfection reagents [12].

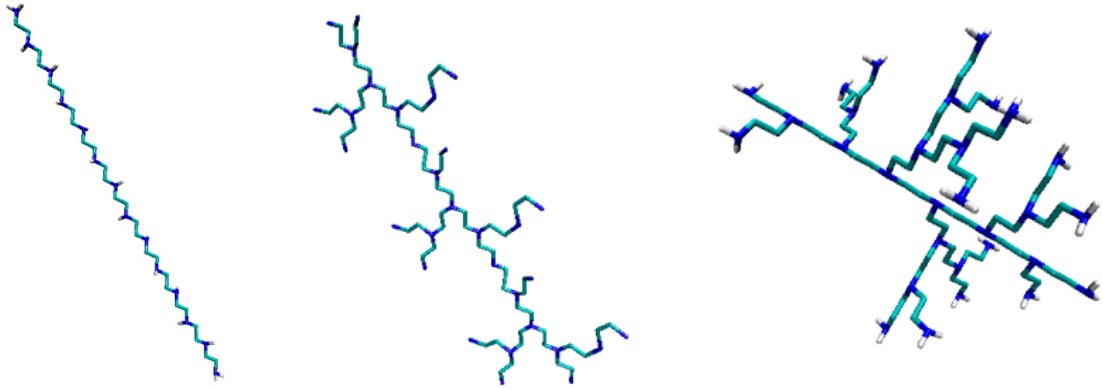

Figure 1. Examples of PEI molecules: linear L (**left**); branched B (**middle**) and dendrimer D (**right**) [13–15].

Calculations at the B3LYP/6-31G (d, p) level of theory [16–19] confirmed the hypothesis that rhombellanes are energetically feasible in the hope of a real synthesis [20–26].

Rhombellanes have certain specific traits which define these group of structures. At first, all strong rings are squares/rhombs. The second vertex classes consist of only non-connected vertices. Omega polynomial has a single term: 1X^|E| and they contain one K2.3 complete bipartite subgraph or the smallest rhombellane rbl.5. The end line graph of the parent graph has a Hamiltonian circuit.

To explore the internal molecular mobility that is important in the bioactivity study of these compounds we used the Molecular mechanics (MMFF94) [27] method. In this way we study the pharmaceutical important parameters of rhombellanes [27].

Rhombellans (Figure 2) seem to be structures suitable for medical chemistry, with a new class of structures which could be an used in personalized medicine as new carrier nanostructures.

Because rhombellane homeomorphs may be bound to a protein, an attempt was made to deposit PEI derivatives on rhombellanes, as possible nano-drug complexes. Detailed analysis of structural properties after docking showed many interesting features. Behavior of polyethylenimine (linear LPEI, branched BPEI and/or dendrimers DPEI) with respect to rhombellane homeomorphs, in terms of their (interacting) topology, geometry and energy, was studied. After the docking procedure, the best values of ligand–rhombellane affinity were found, which is an important result for homeomorphs.

The article is a collection of new data in the new field of rhombellanes (Figure 2).

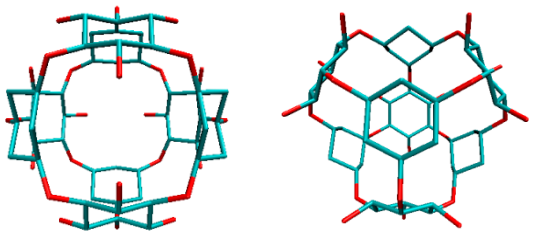

Figure 2. *Cont.*

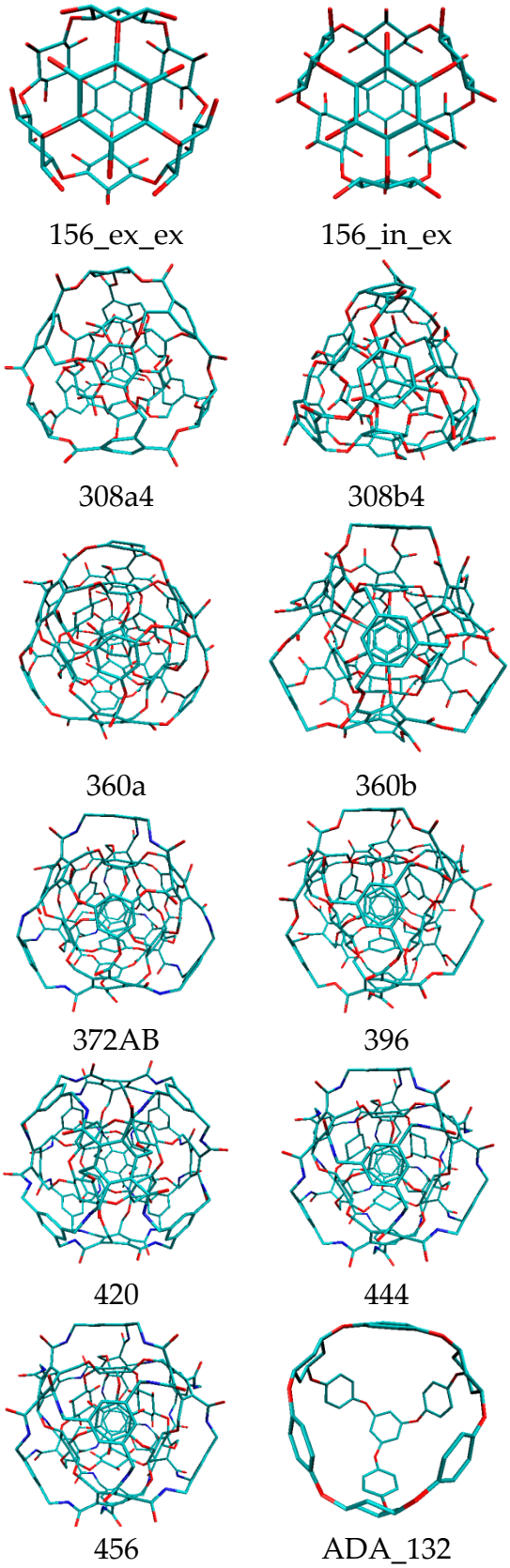

Figure 2. Graphic representation of the cube rhombellanes.

2. Methods

Docking Procedure

The ligand molecule was obtained from others study [1–8,13–15,28–31] Rhombellane homeomorphs, were received from Topo Cluj Group [32], the C60 structure was downloaded from Brookhaven Protein Database PDB [33], while C60 functionalized derivatives were obtained from PubChem database [34].

During the docking stage, there were structures of ligand and nano-systems containing only polar hydrogen atoms. In the case of all nanoparticles, the grid box dimensions were established equal to 26 × 26 × 26 Å, boxing coordinates amount to (0,0,0). All initial procedures related with preparation of ligand and nano-systems during the docking procedure were realized with the use of the AutoDock Tools package [35]. Using the AutoDockVina software in the docking procedure, after assigning hydrogen bonds, the molecules were loaded and stored as pdb-files [36]. The investigated ligands were loaded and their torsions along the rotatable bonds were assigned and next saved as "ligand.pdbqt". The grid menu after loading "pdbqt" was toggled [37]. For the search of ligand–rbl fullerene interactions, the map files were selected directly with setting up the grid points separately for each structure. The Lamarckian genetic algorithm completed the docking parameter files [38]. As a reference structure, the fullerene C60 was used, the most referred to structure in nanoscience.

All calculations during the docking stage were realized with the exhaustiveness parameter equal to 20, since such a value ensures an appropriate reproducibility of the results and a reasonable time of calculation. The structural analysis of considered systems and visualization of obtained complexes were realized with use of the VMD package [39]. The value of binding constant was calculated based on the formula:

$$K_{max} = \exp^{(\frac{-\Delta G_{max}}{RT})}$$

where ΔG max represent maximal value of binding affinity obtained during docking stage, R represent value of gas constant and T temperature.

3. Results and Discussion

The results are presented in the following tables and figures. Rhombellane structures are given by their atom number.

In relation to the ligands of the D and L groups, the largest affinity values of the ligand–fullerenes were found for all ligands from B group (Figure 3, Table 1), for which the affinity values range from −2 to −7 kcal/mol. With the B_1320_PEI_C60N31 ligand the values are the lowest, thus showing the best affinity for all proposed fullerenes, with affinity values from −4 to −7 kcal/mol. All values of the interactions were compared with the values for C_{60} fullerene, which was, as always, used as the reference structure in nanostructures family. Therefore, in all cases of ligands from the B group, there are affinities with better and worse values of energy compared with affinity ligand–fulleren C_{60} (Figure 3, Table 1).

Table 1. The best binding affinity of ligands, BPEI, with the active site of Rbl-nano-structures (first column) during nine conformations.

	Gibbs Free Energy (kcal/mol)				
NANO-STRUCTURES	**B10230_PEI_C22N12**	**B10230_PEI_C44N23**	**B10230_PEI_C20N11**	**B10230_PEI_C40N21**	**B10230_PEI_C60N31**
144_ex_ex	−2.4	−2.9	−2.4	−2.8	−4.4
144_in_ex	−2.3	x	−2.2	−2.7	−4.3
156_ex_ex	−2.4	−2.8	−2.5	−2.6	−4.5
156_in_ex	−2.6	−2.9	−2.6	−2.9	−4.8
308a4	−3.9	−4.8	−3.9	−4.6	−6.4
308b4	−4.1	−5.0	−4.2	−4.6	−6.9
360a	−4.0	−4.5	−3.9	−4.5	−6.5
360b	−3.9	−4.5	−3.7	−4.2	−6.1

Table 1. *Cont.*

Gibbs Free Energy (kcal/mol)					
NANO-STRUCTURES	**B10230_PEI_ C22N12**	**B10230_PEI_ C44N23**	**B10230_PEI_ C20N11**	**B10230_PEI_ C40N21**	**B10230_PEI_ C60N31**
372AB	−4.3	−4.8	−4.0	−4.4	−6.2
396	−3.9	−4.7	−3.9	−4.2	−5.8
420	−4.2	−4.7	−3.7	−4.1	−5.4
444	−3.7	−4.3	−3.6	−4.0	−5.6
456	−3.9	−4.5	−3.5	−4.0	−5.3
ADA_132	−5.0	−4.4	−4.4	−4.2	x
C60	−3.8	−4	−3.8	−3.8	−4.8

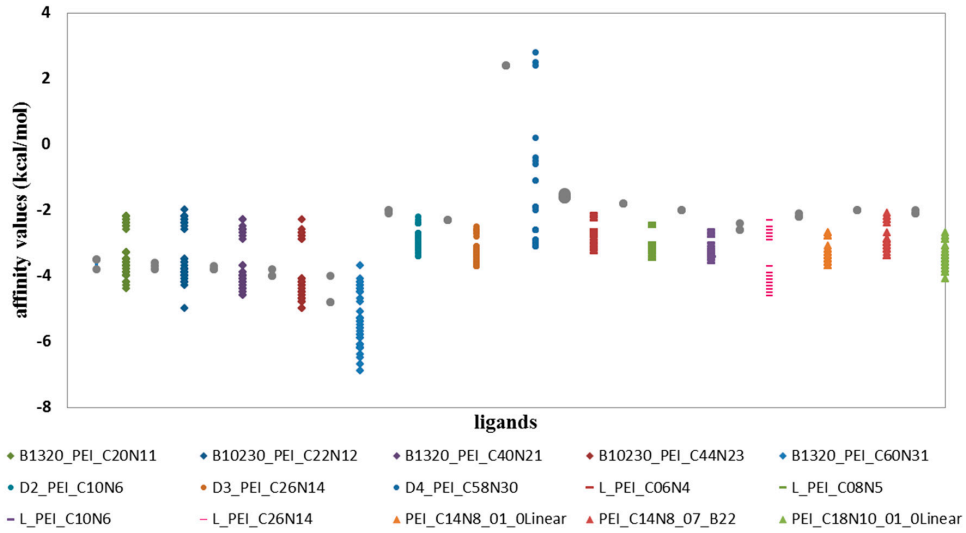

Figure 3. Energy (in kcal/mol) of the affinity ligand (PEI)-Rhombellanes complex (left and right), for B-, D-, and L-PEI; in scale to O kcal/mol.

When comparing the values of affinity of D ligand–fulleren and L ligand–fulleren complexes, it is clear that these complexes show the lowest values with all study fullerenes, compared with fulleren C_{60} (Figure 3, Tables 2 and 3).

Table 2. The best binding affinity of ligands, BPEI, with the active site of Rbl-nano-structures (first column) during nine conformations.

Docked Energy (kcal/mol)			
NANO-STRUCTURES	**D2_PEI_C10N6**	**D3_PEI_C26N14**	**D4_PEI_C58N30**
144_ex_ex	−2.4	−2.6	−2.6
144_in_e	−2.4	−2.8	−2.6
156_ex_ex	−3.1	−3.3	−3
156_in_ex	−3.1	−3.4	−3.1
308a4	−3.1	−3.6	−0.6
308b4	−3.3	−3.7	−2
360a	−3.1	−3.6	−2.9
360b	−2.9	−3.3	2.5
372AB	−3.2	−3.7	−1.1
396	−2.8	−3.6	4.9
420	−2.9	−3.5	5
444	−2.8	−3.3	10.4
456	−2.9	−3.3	8.2
ADA_132	−3.4	−2.7	−1.9
C_{60}	−2.1	−2.3	2.4

Table 3. The best binding energy of ligands, BPEI, with the active site of Rbl-nano-structures (first column) during nine conformations. In letters ABCD, etc., have been marked further nanostructures A-L_PEI_C06N4; B-L_PEI_C08N5; C-L_PEI_C10N6; D-L_PEI_C26N14; E-PEI_C14N8_01_0Linear; F-PEI_C14N8_07_B22; G-PEI_C18N10_01_0Linear.

Gibbs Free Energy (kcal/mol)							
NANO-STRUCTURES	**A**	**B**	**C**	**D**	**E**	**F**	**G**
144_ex_ex	−2.3	−2.5	−2.8	−2.8	−2.8	−2.3	−2.9
144_in_ex	−2.2	−2.5	−2.8	−2.7	−2.8	−2.4	−2.9
156_ex_ex	−2.8	−3.2	−3.4	−2.6	−3.6	−2.9	−3.7
156_in_ex	−2.9	−3.3	−3.5	−2.9	−3.7	−3.2	−3.6
308a4	−3.1	−3.1	−3.4	−4.6	−3.4	−3.1	−3.8
308b4	−3.2	−3.5	−3.4	−4.6	−3.7	−3.4	−4.1
360a	−2.6	−3.1	−3.2	−4.5	−3.6	−3.2	−3.5
360b	−2.8	−3.2	−3.4	−4.2	−3.5	−3.2	−3.5
372AB	−2.7	−3.2	−3.3	−4.4	−3.5	−3.2	−3.8
396	−2.7	−3.2	−3.4	−4.2	−3.4	−3.1	−3.6
420	−2.6	−3.1	−3.4	−4.1	−3.5	−2.9	−3.5
444	−2.8	−3.3	−3.4	−4.0	−3.6	−3.1	−3.4
456	−2.8	−3.3	−3.5	−4	−3.6	−3	−3.6
ADA_132	−3.3	−3.5	−3.5	−4.2	−3.4	−3.4	−3.3
C_{60}	−1.6	−1.8	−2	−2.6	−2.2	−2	−2.1

For the other proposed ligands of type D, L and PEI_C14N8_01_Linear; PEI_C14N8_07_B22; PEI_C18N10_01_0, their affinities ranged from −2 to −4 kcal/mol (Tables 2 and 3). However, the ligand D4_PEI_C58N30 shows not only affinity in this range, i.e., (−2 to −4 kcal/mol), but also low affinities for fullerenes with high values of around 0 kcal/mol, and it does not even have the possibility of interacting with fullerenes as their affinity values are positive (Figure 3, Tables 2 and 3)

The diagram (Figure 4) shows two populations of affinity values of ligand B–fullerenes. The first with values ranging from −2 to −3 kcal/mol and in the case of second population from −3.3 to −5 kcal/mol for B1320_PEI_C20N11; B10230_PEI_C22N12; B1320_PEI_C40N21; B10230_PEI_C44N23.

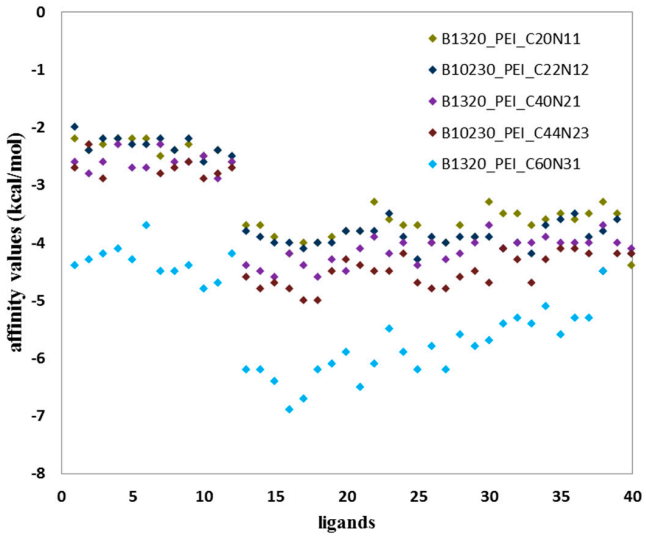

Figure 4. Example of diagram showing two populations of affinity values of ligand B–fullerenes.

Similarly, two populations are visible in the case of B1320_PEI_C60N31 with markedly reduced affinity values relative to the values of the affinity represented by the first four ligands of the B group, described above (Tables 3 and 4). The first population has interaction values ranging from −4 kcal/mol to −5 kcal/mol, the second shows much higher affinity values from −5 to −7 kcal/mol (Tables 3 and 4).

Table 4. The best binding affinity of ligands, BPEI, –columns A. Columns B represent k max values of binding constant estimated with use of binding free energy obtained for the best complex of ligand with nanostructure, while columns C represent k max differences relative C_{60} molecule, defining the difference in quality of ligand binding with considered nanostructure in comparison to reference system.

NANO-STRUCTURES	B10230_PEI C22N12			B10230_PEI C44N23			B10230_PEI C20N11			B10230_PEI C40N21			B10230_PEI C60N31		
	A	**B**	**C**	**A**	**B**	**C**	**A**	**B**	**C**	**A**	**B**	**C**	**A**	**B**	**C**
144_ex_ex	−2.4	57.4	−90.6	−2.9	133.6	−84.4	−2.4	57.4	−90.6	−2.8	112.8	−26.3	−4.4	1679.7	−8.3
144_in_ex	−2.3	48.5	−92.0		1.0	−99.9	−2.2	41.0	−93.3	−2.7	95.3	−28.9	−4.3	1418.9	−10.4
156_ex_ex	−2.4	57.4	−90.6	−2.8	112.8	−86.8	−2.5	68.0	−88.9	−2.6	80.5	−31.6	−4.5	1988.6	−6.3
156_in_ex	−2.6	80.5	−86.8	−2.9	133.6	−84.4	−2.6	80.5	−86.8	−2.9	133.6	−23.7	−4.8	3299.5	0.0
308a4	−4.0	855.1	40.2	−4.6	2354.2	175.3	−3.9	722.3	18.4	−4.6	2354.2	21.1	−6.4	49,120.4	33.3
308b4	−4.1	1012.4	65.9	**−5.0**	**4624.3**	**440.8**	**−4.2**	**1198.5**	**96.4**	**−4.6**	**2354.2**	**21.1**	**−6.9**	**114,226.6**	**43.8**
360a	−4.0	855.1	40.2	−4.5	1988.6	132.5	−3.9	722.3	18.4	**−4.5**	**1988.6**	**18.4**	**−6.5**	**58,151.8**	**35.4**
360b	−3.9	722.3	18.4	−4.5	1988.6	132.5	−3.7	515.4	−15.5	−4.2	1198.5	10.5	−6.1	29,604.6	27.1
372AB	**−4.3**	**1418.9**	**132.5**	**−4.8**	**3299.5**	**285.8**	−4.0	855.1	40.2	−4.4	1679.7	15.8	−6.2	35,047.8	14.6
396	−3.9	722.3	18.4	−4.7	2787.1	225.9	−3.9	722.3	18.4	−4.2	1198.5	10.5	−5.8	17,842.5	29.2
420	−4.2	1198.5	96.4	−4.7	2787.1	225.9	−3.7	515.4	−15.5	−4.1	1012.4	7.9	−5.4	9083.5	20.8
444	−3.7	515.4	−15.5	−4.3	1418.9	65.9	−3.6	435.3	−28.6	−4.0	855.1	2.6	−5.6	12,730.8	12.5
456	−3.9	722.3	18.4	−4.5	1988.6	132.5	−3.5	367.7	−39.7	−4.0	855.1	5.3	−5.3	7672.8	16.7
ADA_132	**−5.0**	**4624.3**	**657.9**	−4.4	1679.7	96.4	**−4.4**	**1679.7**	**175.3**	−4.2	1198.5	5.3		1.0	−6.3
C60	−3.8	610.2	0.0	−4.0	855.1	0.0	−3.8	610.2	0.0	−3.8	610.2	7.9	−4.8	3299.5	−100.0

Two populations are also visible for other ligands from the D and L groups forming interactions with tested fullerenes. Quantitatively, the largest number of ligand–fullerene interactions is expressed by affinity values in the range of −3 to −4 kcal/mol, and this is a representative population. The second population is expressed by a small representation of the number of affinities with values ranging from −2 to −3 kcal/mol.

The existence of these two populations is closely related to the interaction with two fullerene groups. Small structures of ligands easily react with small structures of nanoparticles and vice versa.

Unfortunately, the energy parameter itself is insufficient. By using energy per quantity of carbon atoms (kcal/mol) parameter it is clearly visible that the elongation of carbon chain does not affect the binding efficiency, but only increases affinity (Figure 5).

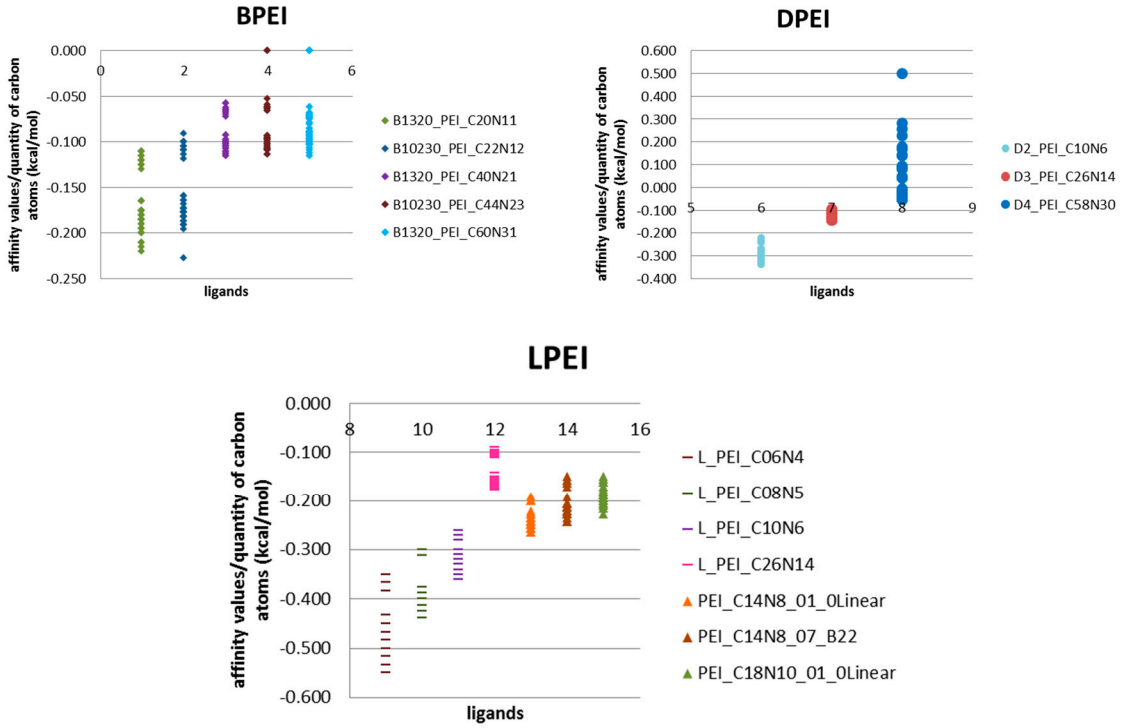

Figure 5. Affinity values per quantity of carbon atoms in kcal/mol for all ligands BPEI, DPEI and LPEI.

The best binding efficiency is shown by linear ligands L, with highest values of this parameter, compared with values of ligands from B and D groups (Figure 5). The shorter the molecule, the better the binding performance, the more the particle grows and the lower the yield. For linear LPEI structures, as the carbon chain length increases, the binding efficiency decreases and the saturation around the length of the chain with twenty carbon atoms is clearly visible (Figure 6).

Similar observations have been made for group B ligands. Twofold chain elongation results in a two-fold decrease in binding efficiency (Figure 5, Table 1). In the case of dendrimeric structures, as the complexity of the system increases, the value of binding efficiency decreases (Figure 5, Table 2). Among the fullerenes tested, the best effects were found for fullerenes ADA and 308a4/b4. Small ligands easily form complexes primarily with fullerene ADA, long-chain ligands interact with the 308a4/b4 nanostructure (Figure 5). Thus, for small ligands, the best binding efficiency is with small fullerenes, while large fullerenes require large ligands.

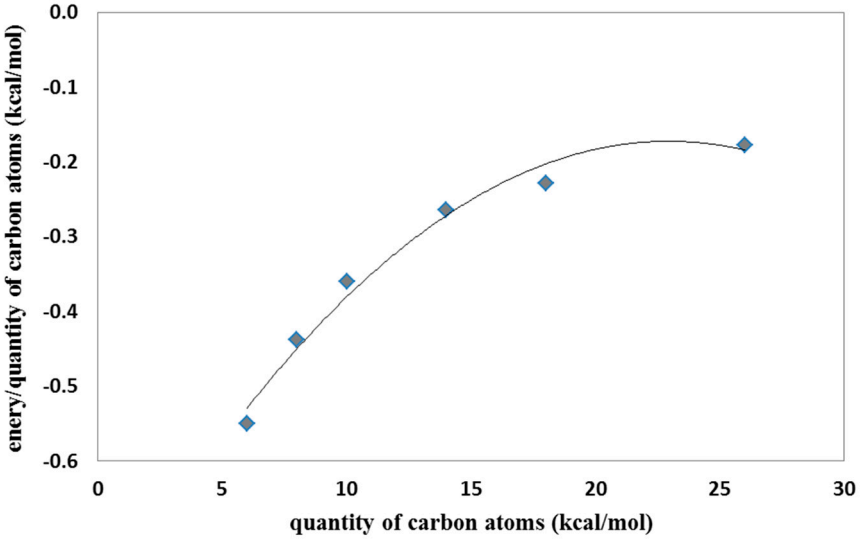

Figure 6. The affinity values per quantity of carbon atoms in function of quantity of carbon atoms for ligands PEI.

The best binding affinity of ligands BPEI (Table 4) DPEI (Table 5) and LPEI (Tables 6 and 7), k max values of binding constant estimated with use of binding free energy obtained for the best complex of ligand with nanostructure and k max differences relative C_{60} molecule, defining the difference in the quality of ligand binding with considered nanostructure in comparison to reference system, were estimated for the tested Rbl-structures in relation to the affinity value obtained for the fullerene C_{60}. The highest positive percentage deviations from the affinity of ligands to fullerene C_{60} were obtained for those Rbl-structures showing the highest binding values (Tables 4–7, in boldface). Two last columns show the equilibrium K value of the bonds.

Table 5. The best binding affinity of ligands, BPEI, –columns A. Columns B represent k max values of binding constant estimated with use of binding free energy obtained for the best complex of ligand with nanostructure, while columns C represent k max differences relative C_{60} molecule, defining the difference in quality of ligand binding with considered nanostructure in comparison to reference system.

NANO-STRUCTURES	D2_PEI_C10_N6			D3_PEI_C26_N14			D4_PEI_C58_N30		
	A	B	C	A	B	C	A	B	C
144_ex_ex	−2.4	57.44118	65.9216	−2.6	80.50545	65.9216	−2.6	80.50545	462,332.8
144_in_ex	−2.4	57.44118	65.9216	−2.8	112.8307	132.5439	−2.6	80.50545	462,332.8
156_ex_ex	−3.1	187.2105	440.7664	−3.3	262.3808	440.7664	−3	158.1354	908,248.5
156_in_ex	−3.1	187.2105	440.7664	−3.4	310.6226	540.1927	**−3.1**	**187.2105**	**1,075,259**
308a4	−3.1	187.2105	440.7664	−3.6	435.3464	797.2483	−0.6	2.752998	15,713.54
308b4	**−3.3**	**262.3808**	**657.8996**	**−3.7**	**515.39**	**962.2179**	−2	29.24283	167,874.3
360a	−3.1	187.2105	440.7664	**−3.7**	**515.39**	**962.2179**	**−2.9**	**133.5759**	**767,175.8**
360b	−2.9	133.5759	285.8405	−3.3	262.3808	440.7664	2.5	0.014705	−15.5307
372AB	−3.2	221.6313	540.1927	**−3.7**	**515.39**	**962.2179**	−1.1	6.401927	36,673.42
396	−2.8	112.8307	225.9168	−3.6	435.3464	797.2483	4.6	0.000425	−97.5601
420	−2.9	133.5759	285.8405	−3.5	367.7342	657.8996	5	0.000216	−98.7578
444	−2.8	112.8307	225.9168	−3.3	262.3808	440.7664	10.4	2.38E−08	−99.9999
456	−2.9	133.5759	285.8405	−3.3	262.3808	440.7664	8.2	9.76E−07	−99.9944
ADA_132	**−3.4**	**310.6226**	**797.2483**	−2.7	95.30732	96.42822	−1.9	24.70122	141,786.7
C60_2	−2.1	34.61947	0	−2.3	48.52017	0	2.4	0.017409	0

Table 6. The best binding affinity of ligands, BPEI, –columns A. Columns B represent k max values of binding constant estimated with use of binding free energy obtained for the best complex of ligand with nanostructure, while columns C represent k max differences relative C_{60} molecule, defining the difference in quality of ligand binding with considered nanostructure in comparison to reference system.

NANO-STRUCTURES	L_PEI_C06N4			L_PEI_C08N5			L_PEI_C10N6			L_PEI_C26N14		
	A	**B**	**C**	**A**	**B**	**C**	**A**	**B**	**C**	**A**	**B**	**C**
144_ex_ex	−2.3	48.5	225.9	−2.5	68.0	225.9	−2.8	112.8	285.	−2.8	112.8	40.2
144_in_ex	−2.2	41.0	175.3	−2.5	68.0	225.9	−2.8	112.8	285.8	−2.7	95.3	18.4
156_ex_ex	−2.8	112.8	657.9	−3.2	221.6	962.2	−3.4	310.6	962.2	−2.6	80.5	0.0
156_in_ex	−2.9	133.6	797.2	−3.3	262.4	1157.5	**−3.5**	**367.7**	1157.5	−2.9	133.6	65.9
308a4	−3.0	158.1	962.2	−3.3	262.4	1157.5	−3.4	310.6	962.2	**−4.6**	**2354.2**	**2824.3**
308b4	**−3.2**	**221.6**	**1388.7**	**−3.5**	**367.7**	**1662.4**	−3.4	310.6	962.2	**−4.6**	**2354.2**	**2824.3**
360a	−2.7	95.3	540.2	−3.1	187.2	797.2	−3.2	221.6	657.9	−4.5	1988.6	2370.1
360b	−2.8	112.8	657.9	−3.2	221.6	962.2	−3.4	310.6	962.2	−4.2	1198.5	1388.7
372AB	−2.7	95.3	540.2	−3.2	221.6	962.2	−3.4	310.6	962.2	−4.4	1679.7	1986.5
396	−2.7	95.3	540.2	−3.2	221.6	962.2	−3.4	310.6	962.2	−4.2	1198.5	1388.7
420	−2.7	95.3	540.2	−3.1	187.2	797.2	**−3.6**	**435.3**	**1388.7**	−4.1	1012.4	1157.5
444	−2.8	112.8	657.9	−3.3	262.4	1157.5	−3.4	310.6	962.2	−4.0	855.1	962.2
456	−2.8	112.8	657.9	−3.3	262.4	1157.5	**−3.5**	**367.7**	**1157.5**	−4.0	855.1	962.2
ADA_132	**−3.3**	**262.4**	**1662.4**	**−3.5**	**367.7**	**1662.4**	**−3.5**	**367.7**	**1157.5**	−4.2	1198.5	1388.7
C60	−1.6	14.9	0.0	−1.8	20.9	0.0	−2.0	29.2	0.0	−2.6	80.5	0.0

Table 7. The best binding affinity of ligands, BPEI, –columns A. Columns B represent k max values of binding constant estimated with use of binding free energy obtained for the best complex of ligand with nanostructure, while columns C represent k max differences relative C_{60} molecule, defining the difference in quality of ligand binding with considered nanostructure in comparison to reference system.

NANO-STRUCTURES	PEI_C14N8_01_0Linear			PEI_C14N8_07_B22			PEI_C18N10_01_0Linear		
	A	**B**	**C**	**A**	**B**	**C**	**A**	**B**	**C**
144_ex_ex	−2.8	112.8307	40.15285	−2.3	48.52017	175.2998	−2.9	133.5759	37.5
144_in_ex	−2.8	112.8307	65.9216	−2.4	57.44118	225.9168	−2.9	133.5759	37.5
156_ex_ex	−3.6	435.3464	225.9168	−2.9	133.5759	657.8996	−3.7	515.39	62.5
156_in_ex	**−3.7**	**515.39**	**657.8996**	−3.2	221.6313	1157.519	−3.7	515.39	75
308a4	−3.2	221.6313	440.7664	−3.1	187.2105	1388.729	−3.7	515.39	87.5
308b4	**−3.7**	**515.39**	**540.1927**	**−3.4**	**310.6226**	**2824.283**	**−4.1**	**1012.371**	**93.75**
360a	−3.6	435.3464	440.7664	−3.2	221.6313	962.2179	−3.5	367.7342	62.5
360b	−3.5	367.7342	356.7818	−3.2	221.6313	797.2483	−3.5	367.7342	68.75
372AB	−3.5	367.7342	657.8996	−3.2	221.6313	1662.449	**−3.8**	**610.1504**	68.75
396	−3.4	310.6226	440.7664	−3.1	187.2105	1157.519	−3.6	435.3464	68.75
420	−3.5	367.7342	440.7664	−3	158.1354	962.2179	−3.5	367.7342	68.75
444	−3.6	435.3464	356.7818	−3.1	187.2105	797.2483	−3.4	310.6226	75
456	−3.6	435.3464	440.7664	−3	158.1354	1157.519	−3.6	435.3464	68.75
ADA_132	−3.4	310.6226	797.2483	**−3.4**	**310.6226**	440.7664	−3.3	262.3808	100
C60	−2.2	40.98466	0	−2	29.24283	0	−2.1	34.61947	0

The higher the K value, the more the reaction proceeds towards the formation of the complex.

Detailed analysis of structural properties after docking showed that the affinities of the ligands to the rhombellanes surface are correlated with the quality of hydrogen bonds formed between them. The distance between acceptor and hydrogen atoms is the criterion for classification of the strength of hydrogen bonds: weak interactions are characterized by distances <3 Å, strong interactions by a distance <1.6 Å and medium strength by values in the range from 1.6 Å to 2.0 Å.

Ligand B1320_PEI_C20N11 and nanostructure ADA_132 form two hydrogen bonds with medium strength between amino groups of ligand and oxygen atoms of fullerenes with binding lengths 2.79Å and 2.95Å (Figure 7). Also, in the case of ligand B1320_PEI_C60N31–fullerene 308b4 four medium hydrogen bonds were created with bond lengths 2.69 Å, 2.87 Å and 2.93 Å (Figure 7).

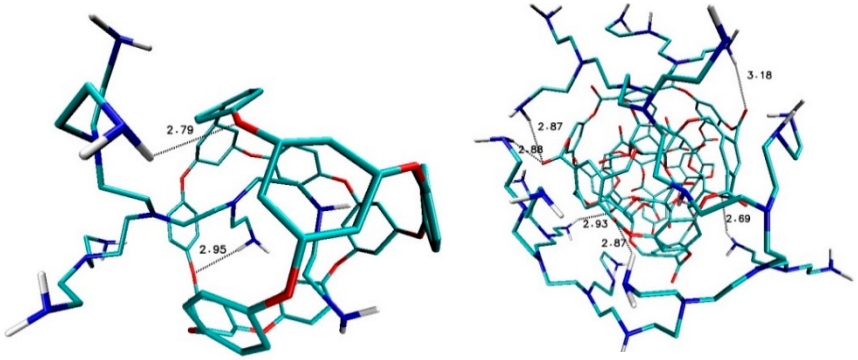

Figure 7. Interactions found in the complexes of fullerene ADA_132 and ligands B1320_PEI_C20N11 (**left**) and fullerene 308b4 with ligand B1320_PEI_C60N31 (**right**) after the docking procedure.

After the docking of ligands from D group, different interactions could be found, namely in the case of fullerene ADA_132 and ligands D2_PEI_C10N6 there is only one week hydrogen bond, while for fullerene 308b4 with D3_PEI_C26N14 ligand there are several strong and medium hydrogen bonds, first of all between amino groups of ligand and oxygen atom of nanostructure with bond lengths 1.9 Å, 2.47 Å., 2.52 Å and 2.94 Å. In the case of fullerene 156_in_ex with ligand D4_PEI_C58N30, there are three hydrogen bonds of medium strength; with bond lengths 2.50 Å, 2.80 Å and 2.83 Å (Figure 8).

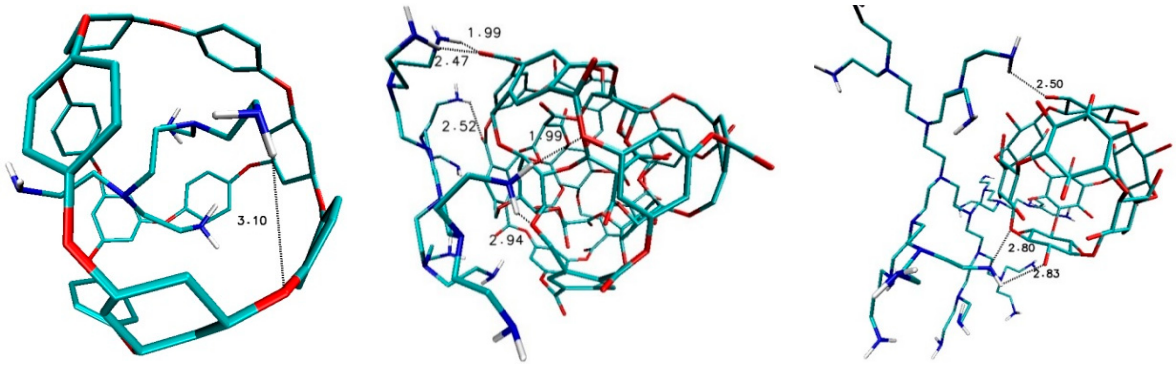

Figure 8. Interactions found in the complexes of fullerene ADA_132 and ligands D2_PEI_C10N6 (**left**) and fullerene 308b4 with D3_PEI_C26N14 ligand (**middle**) and 156_in_ex with ligand D4_PEI_C58N30 (**right**) after the docking procedure.

After the docking of ligands from L group, different interactions were also found, namely in the case of fullerene ADA_132 and ligands L_PEI_C10N6 there is only one-week hydrogen bond, the same as in the case D2_PEI_C10N6-ADA_132 (Figure 9). Again, as in DPEI-308b4 case, there are many interactions between hydrogen atoms of nitrogen groups of ligand and oxygen atoms of nanostructure with values 1.99 Å, 2.47 Å, 2.52 Å, 2.94 Å and 3.05 Å (Figure 9).

In the case of fullerene 308b4 and ligand PEI_C18N10_01_0Linear, there are several strong and medium hydrogen bonds, while in the case of fullerene C_{60} as references structure with B1320_PEI_C60N31 ligand there are no important interactions (Figure 10).

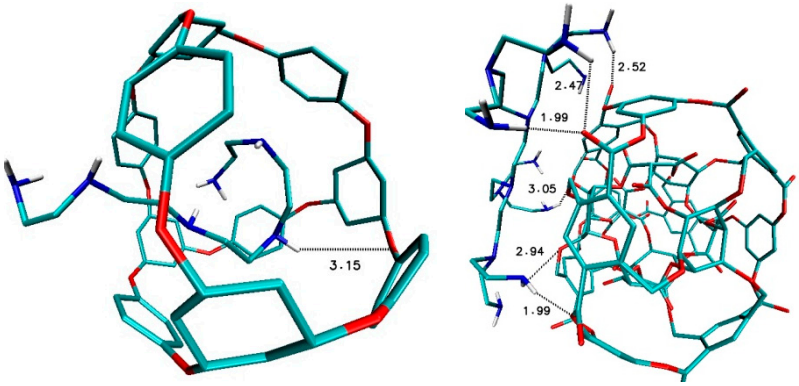

Figure 9. Interactions found in the complexes of fullerene ADA_132 and ligands L_PEI_C10N6 (**left**) and fullerene 308b4 with ligand L_PEI_C26N14 (**right**) after the docking procedure.

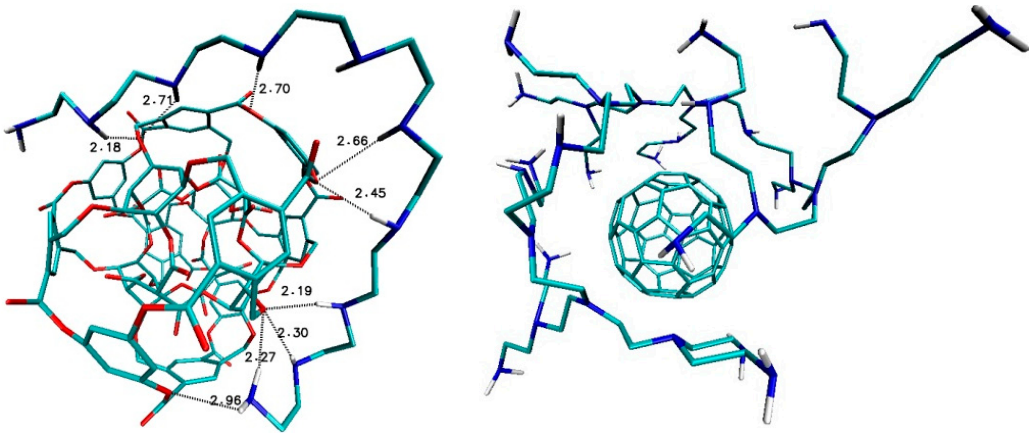

Figure 10. Interactions found in the complexes of fullerene 308b4 and ligands PEI_C18N10_01_0Linear (**left**) and fullerene c60 as references structure with ligand B1320_PEI_C60N31 (**right**) after the docking procedure.

4. Conclusions

As a proposal for a new nanodrug, an attempt was made to implement PEI ligands on the cube rhombellane homeomorphic surface. Fourteen types of cube rhombellanes were used together with three groups of polyethylenimines (PEIs), namely, branched (B-PEI), linear (L-PEI) and dendrimer (D-PEI). Ligand-fullerenes interactions were described in terms of quality and quantity. Specifically, there were calculated the affinity values and affinity per quantity of carbon atoms after the docking procedure for ligand nanostructure. The best binding efficiency was shown by linear ligands L, with highest values of this parameter, compared with values of ligand from B and D groups. The shorter the molecule, the better the binding performance, the more the particle grows and the lower the yield. For linear structures LPEI, as the carbon chain length increases, the binding efficiency decreases and the saturation around the length of the chain with twenty carbon atoms is clearly visible. Similar observations have been made for group B ligands. Twofold chain elongation results in a two-fold decrease in binding efficiency. In the case of dendrimeric structures, as the complexity of the system increases, the value of binding efficiency decreases. Two populations of affinity values have been observed, which is closely related to the interaction with two fullerene groups. Small structures of ligands easily react with small structures of nanoparticles and vice versa. The best binding affinity of ligands and k max values of binding constant were estimated with the use of binding free energy obtained for the best complex of ligand with nanostructure. Also, k max differences relative C_{60} molecule, defining the difference in quality of ligand binding with considered nanostructure in comparison to reference system, were calculated. The highest positive percentage deviations were

obtained for ligand–fullerene complexes showing the highest binding energy values. Detailed analysis of structural properties after docking showed that the values of affinity of the studied indolizine ligands to the Rhombellanes surface are correlated with the strength/length of hydrogen bonds formed between them.

Author Contributions: Conceptualization, B.S.; Methodology, B.S. and P.C.; Validation, B.S. and P.C.; Formal Analysis, B.S.; Investigation, B.S.; Resources, B.S.; Data Curation, B.S.; Writing—Original Draft Preparation, B.S.; Writing—Review & Editing, B.S. and P.C.; Visualization, B.S. and P.C.; Supervision, B.S.; Project Administration, B.S.; Funding Acquisition, B.S.

Funding: This research received no external funding.

Acknowledgments: Thanks for fruitful cooperation for many years to MV Diudea; this article was supported by PL-Grid Infrastructure (http://www.plgrid.pl/en).

Conflicts of Interest: The authors declare no conflict of interest.

References and Note

1. Lungu, C.L.; Diudea, M.V.; Putz, M.V.; Grudzinski, I.P. Linear and Branched PEIs (Polyethylenimines) and Their Property Space. *Int. J. Mol. Sci.* **2016**, *17*, 555. [CrossRef]
2. Szefler, B.; Diudea, M.V.; Grudziński, I.P. Nature of Polyethyleneimine-Glucose Oxidase interactions. *Stud. Univ. Babes-Bolyai Chem.* **2016**, *61*, 249–260.
3. Szefler, B.; Diudea, M.V.; Putz, M.V.; Grudziński, I.P. Molecular Dynamic Studies of the Complex Polyethylenimine and Glucose Oxidase. *Int. J. Mol. Sci.* **2016**, *17*, 1796. [CrossRef]
4. Szefler, B.; Czeleń, P.; Diudea, M.V. Docking of Indolizine derivatives on cube Rhombellane functionalized Homeomorphs. *Stud. Univ. Babes-Bolyai Chem.* **2018**, *63*, 7–18. [CrossRef]
5. Czeleń, P. Investigation of the Inhibition Potential of New Oxindole Derivatives and Assessment of Their Usefulness for Targeted Therapy. *Symmetry* **2019**, *11*, 974. [CrossRef]
6. Czeleń, P.; Szefler, B. The Immobilization of ChEMBL474807 Molecules Using Different Classes of Nanostructures. *Symmetry* **2019**, *11*, 980. [CrossRef]
7. Czeleń, P.; Szefler, B. The Immobilization of Oxindole Derivatives with Use of Cube Rhombellane Homeomorphs. *Symmetry* **2019**, *11*, 900. [CrossRef]
8. Szefler, B.; Czeleń, P. Docking of Cisplatin on Fullerene Derivatives and Some Cube Rhombellane Functionalized Homeomorphs. *Symmetry* **2019**, *11*, 874. [CrossRef]
9. Astruc, D.; Boisselier, E.; Ornelas, C. Dendrimers Designed for Functions: From Physical, Photophysical, and Supramolecular Properties to Applications in Sensing, Catalysis, Molecular Electronics, and Nanomedicine. *Chem. Rev.* **2010**, *110*, 1857–1959. [CrossRef]
10. Vögtle, F.; Richardt, G.; Werner, N. *Dendrimer Chemistry Concepts, Syntheses, Properties, Applications*; John Wiley & Sons: Hoboken, NJ, USA, 2009; ISBN 3-527-32066-0.
11. Akinc, A.; Thomas, M.; Klibanov, A.M.; Langer, R. Exploring polyethylenimine-mediated DNA transfection and the proton sponge hypothesis. *J. Gene Med.* **2004**, *7*, 657–666. [CrossRef]
12. Rudolph, C.; Lausier, J.; Naundorf, S.; Müller, R.H.; Rosenecker, J. In vivo gene delivery to the lung usingpolyethylenimine and fractured polyamidoamine dendrimers. *J. Gene Med.* **2000**, *2*, 269–278. [CrossRef]
13. Poplawska, M.; Bystrzejewski, M.; Grudzinski, I.P.; Cywinska, M.A.; Ostapko, J.; Cieszanowski, A. Immobilization of gamma globulins and polyclonal antibodies of class IgG onto carbon-encapsulated iron nanoparticles functionalized with various surface linkers. *CARBON* **2014**, *74*, 180–194. [CrossRef]
14. Karachevtsev, V.A.; Glamazda, A.Y.U.; Zarudnev, E.S.; Karachevtsev, M.V.; Leontiev, V.S.; Linnik, A.S.; Lytvyn, O.S.; Plokhotnichenko, A.M.; Stepanian, S.G. Glocose oxidase immobilization onto carbonnanotube networking. *Ukr. J. Phys.* **2012**, *57*, 700.
15. Kasprzak, A.; Popławska, M.; Bystrzejewski, M.; Łabędź, O.; Grudziński, I.P. Conjugation of polyethylenimine and its derivatives to carbon-encapsulated iron nanoparticles. *R. Soc. Chem. Adv.* **2015**, *5*, 85556. [CrossRef]
16. Gomes, J.A.N.F.; Mallion, R.B. Aromaticity and ring currents. *Chem. Rev.* **2001**, *101*, 1349–1383. [CrossRef]
17. Cyrański, M.K.; Krygowski, T.M.; Katritzky, A.R.; Schleyer, P.V.R. To what extent can aromaticity be defined uniquely? *J. Org. Chem.* **2002**, *67*, 1333–1338.

18. Chen, Z.; Wannere, C.S.; Crominboeuf, C.; Puchta, R.; Schleyer, R.V.P. Nucleus-independent chemical shifts (NICS) as an aromaticity criterion. *Chem. Rev.* **2005**, *105*, 3842–3888. [CrossRef]
19. Diudea, M.V.; Lungu, C.N.; Nagy, C.L. Cube-rhombellane related structures: A drug perspective. *Molecules* **2018**, *23*, 2533. [CrossRef]
20. Pauling, L.; Wheland, G.W. The nature of the chemical bond. V. The quantum mechanical calculation of the resonance energy of benzene and naphthalene and the hydrocarbon free radicals. *J. Chem. Phys.* **1933**, *1*, 362–374. [CrossRef]
21. Daudel, R.; Lefebre, R.; Moser, C. *Quantum Chemistry*; Interscienc: New York, NY, USA, 1959.
22. Diudea, M.V.; Cataldo, F. Functionalized rhombellanes in Drug Design. *Curr. Comput.-Aided Drug Des.* **2018**. accepted.
23. Pop, R.; Medeleanu, M.; Diudea, M.V.; Szefler, B.; Cioslowski, J. Fullerenes patched by flowers. *Cent. Eur. J. Chem.* **2013**, *11*, 527–534. [CrossRef]
24. Frisch, M.J.; Trucks, G.W.; Schlegel, H.B.; Scuseria, G.E.; Robb, M.A.; Cheeseman, J.R.; Scalmani, G.; Barone, V.; Mennucci, B.; Petersson, G.A.; et al. *Gaussian 09, Revision, A.1*; Gaussian, Inc.: Wallingford, CT, USA, 2009.
25. Randić, M. Aromaticity of polycyclic conjugated hydrocarbons. *Chem. Rev.* **2003**, *103*, 3449–3605. [CrossRef] [PubMed]
26. Diudea, M.V.; Nagy, C.L. *Periodic Nanostructures*; Springer: Dordrecht, The Netherlands, 2007.
27. Pauling, L. *The Nature of the Chemical Bond University*; Cornell University Press: Ithaca, NY, USA, 1960; Volume 260.
28. Kasprzak, A.; Grudziński, I.P.; Bamburowicz-Klimkowska, M.; Parzonko, A.; Gawlak, M.; Poplawska, M. New insight into Synthesis and Biological Activity of the Polymeric Materials Consisting of Folic Acid and β-cyclodextrin. *Macromol. Biosci.* **2018**, *18*, 1700289. [CrossRef] [PubMed]
29. Kasprzak, A.; Poplawska, M.; Bystrzejewski, M.; Grudzinski, I.P. Sulfhydrylated graphene-encapsulated iron nanoparticles directly aminated with polyethylenimine: A novel magnetic nanoplatform for bioconjugation of gamma globulins and polyclonal antibodies. *J. Mater. Chem. B* **2016**, *4*, 5593. [CrossRef]
30. Bamburowicz-Klimkowska, M.; Poplawska, M.; Grudzinski, I.P. Nanocomposites as biomolecules delivery agents in nano-medicine. *J. Nanobiotechnol.* **2019**, *17*, 48. [CrossRef]
31. Kowalczyk, A.; Sęk, J.P.; Kasprzak, A.; Popławska, M.; Grudzinski, I.P.; Nowicka, A.M. Occlusion phenomenon of redox probe by protein asa way of voltammetric detection of non-electroactive C-reactive protein. *Biosens. Bioelectron.* **2018**, *117*, 232–239. [CrossRef] [PubMed]
32. Topo-Cluj—International scientific group created by prof. M.V. Diudea, Babes-Bolyai University, Faculty of Chemistry and Chemical Engineering, Cluj-Napoca, Romania
33. Kim, K.-H.; Ko, D.K.; Kim, Y.-T.; Kim, N.H.; Paul, J.; Zhang, S.-Q.; Murray, C.B.; Acharya, R.; Kim, Y.H.; DeGrado, W.F.; et al. Protein-directed self-assembly of a fullerene crystal. *Nat. Commun.* **2016**, *7*, 11429. [CrossRef] [PubMed]
34. PubChem. Available online: https://pubchem.ncbi.nlm.nih.gov/May (accessed on 12 May 2019).
35. Shoichet, B.K.; Kuntz, I.D.; Bodian, D.L. Molecular docking using shape descriptors. *J. Comput. Chem.* **2004**, *13*, 380–397. [CrossRef]
36. Trott, O.; Olson, A.J. AutoDock Vina: Improving the speed and accuracy of docking with a new scoring function, efficient optimization, and multithreading. *J. Comput. Chem.* **2010**, *31*, 455–461. [CrossRef]
37. Dhananjayan, K.; Kalathil, K.; Sumathy, A.; Sivanandy, P. A computational study on binding affinity of bio-flavonoids on the crystal structure of 3-hydroxy-3-methyl-glutaryl-CoA reductase—An insilico molecular docking approach. *Der Pharma Chem.* **2014**, *6*, 378–387.
38. Abagyan, R.; Totrov, M. High-throughput docking for lead generation. *Curr. Opin. Chem. Biol.* **2001**, *5*, 375. [CrossRef]
39. Humphrey, W.; Dalke, A.; Schulten, K. VMD: Visual molecular dynamics. *J. Mol. Graph.* **1996**, *14*, 33–38. [CrossRef]